Published in final edited form as:
Microvasc Res. 2013 November ; 90: . doi:10.1016/j.mvr.2013.07.010.

Aligned Human Microvessels Formed in 3D Fibrin Gel by Constraint of Gel Contraction

Kristen T. Morin[a], **Annie O. Smith**[b], **George E. Davis**[b], and **Robert T. Tranquillo**[a,c,*]

[a]Department of Biomedical Engineering, University of Minnesota, 7-105 Nils Hasselmo Hall, 312 Church Street SE, Minneapolis, MN 55455, USA

[b]Department of Medical Pharmacology and Physiology, University of Missouri, MA415 Medical Sciences Building, One Hospital Drive, Columbia, MO 65212, USA

[c]Department of Chemical Engineering & Materials Science, University of Minnesota, 151 Amundson Hall, 421 Washington Ave. SE, Minneapolis, MN 55455, USA

Abstract

This study aimed to form microvessels in fibrin gels, which is of interest both for studying the fundamental cell-matrix interactions as well as for tissue engineering purposes, and to align the microvessels, which would provide natural inlet and outlet sides for perfusion. The data reported here demonstrate the formation of highly interconnected microvessels in fibrin gel under defined medium conditions and the ability to align them using two methods, both of which involved anchoring the gel at both ends to constrain the cell-induced compaction. The first method used only defined medium and resulted in moderate alignment. The second method used defined and serum-containing media sequentially to achieve high levels of microvessel alignment.

Keywords

Vasculogenesis; Fibrin; Alignment; Microvasculature; Defined Medium; HUVECs; Pericytes

Introduction

The need for engineered microvasculature to overcome oxygen diffusion limitations in engineered tissues *in vitro* has been well established (Kaully et al., 2009). In addition, engineered microvasculature would be of use for studying endothelial behavior in controlled environments. Therefore, many researchers are investigating methods for producing engineered microvasculature *in vitro*. Several groups have demonstrated the ability of endothelial cells (ECs) to form monolayers on the inner surfaces of pre-formed tubes within a 3-dimensional scaffold (Price et al., 2010; Zheng et al., 2012). Other investigators have studied the ability of ECs to sprout into 3-dimensional scaffolds from monolayers on the

*Corresponding Author: 7-114 Nils Hasselmo Hall, 312 Church Street SE, Minneapolis, MN 55455, Phone: 612-625-6868, Fax: 612-626-6583, tranquil@umn.edu.
KT Morin: that0028@umn.edu; AO Smith: smithao@health.missouri.edu; GE Davis: davisgeo@health.missouri.edu

Conflict of Interest
None declared.

scaffold surface (Collen et al., 2003; Stratman et al., 2011; Vera et al., 2008), monolayers on embedded microspheres (Ghajar et al., 2008; Grainger and Putnam, 2011), or aggregates of ECs (Korff and Augustin, 1999; Morin and Tranquillo, 2011). However, the method most promising for achieving this goal is the vasculogenic self-assembly of ECs distributed throughout a scaffold into a network of microvessels. Many recent studies have been successful in creating highly interconnected networks (Chen et al., 2010; Davis et al., 2011; Koh et al., 2008; Nakatsu and Hughes, 2008; Rao et al., 2012; Stratman et al., 2009), including a set of studies whereby human umbilical vein ECs (HUVECs) and pericytes (PCs) formed extensive networks in type I collagen gels under defined medium conditions (Stratman et al., 2009, 2010, 2011).

Many support cell types have been utilized in the self-assembly approach to microvascular network formation, including fibroblasts (Chen et al., 2010), mesenchymal stem cells (MSCs; Rao et al., 2012), and PCs (Stratman et al., 2009). Although all of these cell types have been shown to improve EC network formation, PCs are a natural choice due to their association with native capillaries. *In vivo*, PCs are recruited to newly formed capillaries via PDGF-BB and HB-EGF (Bjarnegård et al., 2004; Stratman et al., 2010) and are essential to the maintenance of capillaries (Benjamin et al., 1998). Pericyte recruitment to EC-lined tubes increases vascular basement membrane assembly due to contributions from both cell types (Stratman et al., 2009; Stratman and Davis, 2012;). Additionally, the presence of PCs prevents the dilation of capillaries beyond their physiologic diameters of 5-10 μm (Hellström et al., 2001; Stratman et al., 2009). The advantages of using PCs rather than fibroblasts or MSCs for applications in EC biology are clear, as the presence of PCs more closely mimics the *in vivo* environment.

The majority of research on self-assembled EC networks has involved the use of serum. Serum introduces uncontrolled variables, which causes experimental variability and makes it difficult to elucidate biological mechanisms. For these reasons, a series of studies, including this one, have utilized serum-free conditions (Davis and Camarillo, 1996; Koh et al., 2008; Stratman et al., 2009).

Our previously published system of HUVECs and PCs in collagen I gel (Stratman et al., 2009) meets the above criteria for the ideal engineered microvasculature, but has the disadvantage of a limited potential as a scaffold for engineered tissues. Collagen gels are weak and yield only limited production of additional collagen. Fibrin gels, in contrast, are also initially weak, but entrapped tissue cells degrade the fibrin and produce an abundance of extracellular matrix including mature collagen I (Clark et al., 1995; Grassl et al., 2002) which ultimately leads to tissues strong enough for implantation (Syedain et al., 2011). The results presented here demonstrate the ability of HUVECs and PCs to form fully interconnected microvascular networks in fibrin gel using defined medium.

In addressing oxygen diffusion limitations in tissue engineering, fluid flow through engineered microvasculature will also be required. To achieve true perfusion, microvessel alignment is also necessary to provide natural inlet and outlet sides for flow, as found in tissues such as muscle (Caulfield and Janicki, 1997). Recent work has indicated that mechanically constrained cell-induced gel compaction is an effective means to align microvessels sprouting from EC aggregates during angiogenesis (Morin and Tranquillo, 2011). The studies reported here harness this mechanism in a vasculogenic system, demonstrating the ability to create highly interconnected aligned microvessels via cell-induced gel compaction following microvessel self-assembly.

Studies first assessed the effects of medium composition and PCs on the growth of HUVEC networks in fibrin gel. Then the effects of fibrin gel geometry and compaction on the

HUVEC network alignment in defined medium were examined. Finally, a hybrid approach of sequential use of defined and serum-containing media was explored as a means to further improve network properties.

Methods

Cell Culture

Human umbilical vein ECs (HUVECs; Lonza) were grown in M199 (Gibco) with FBS (Gibco), endothelial cell growth supplement (ECGS; isolated in house from bovine hypothalamus (Maciag, Cerundolo, Ilsley, Kelley, & Forand, 1979)) and heparin salt (Sigma) and used at passages 3-5. Approximately 16 hours prior to casting, the HUVECs were primed (Stratman et al., 2011) using M199 with FGF-2 (R&D Systems), VEGF (R&D Systems) and reduced serum supplement (RSII), prepared as described (Koh et al., 2008).

Human brain pericytes (PCs; ScienCell) were transfected with GFP using lentiviral methods and cultured in DMEM (Gibco) with FBS (Gibco). Passages 6-8 were used.

Isotropic Construct Preparation

Fibrin gels (18 μl) containing HUVECs with or without PCs were cast in the wells of 96-well half-area plates. Final concentrations were 3 million/ml HUVECs and 0.6 million/ml PCs where applicable. The fibrin formulation included 7.5 mg/ml plasminogen-depleted fibrinogen (CalBiochem), 75 μg/ml fibronectin (Sigma), 150 ng/ml of each of stem cell factor, interleukin 3, FLT3 ligand, stromal derived factor, and FGF-2 (all R&D Systems), and 2.75 U/ml thrombin (Sigma). Gels were covered with either defined medium, which consisted of M199 with 4 μl/ml RSII, 40 ng/ml FGFb, 50 μg/ml ascorbic acid (Sigma), and 2 KIU/ml aprotinin (Sigma), or “EGM-2+,” which consisted of EGM-2 (Lonza) with an additional 8% FBS, and cultured for 3 days.

Aligned Construct Preparation

The same fibrin formulation and cell densities were used to cast constructs in slab geometries. A rectangle of fibrin was cast in a plate between two anchoring porous spacers, and the length of the rectangle was varied to create slabs of aspect ratios (length/width) 1.5, 3 and 4.5 (gel volumes were 50, 100, and 150 μl, respectively). After 1-3 days of culture in defined medium, the fibrin was detached from the plate, enabling cellular traction forces to compact and align the fibrin fibrils. Compacted tissues were harvested at day 6, and control slabs were harvested at day 3, prior to detachment.

Compaction Studies

Slabs of aspect ratio 1.5 were cultured as described above with 3 days of defined medium followed by 3 days of test medium. On day 6 of culture, the width across the middle of each slab was measured. A reduction in slab width was indicative of gel compaction. Test media included defined medium with TGF-β1 (R&D Systems), defined medium with supplements from the EGM-2 bullet-kit (includes VEGF, bFGF-2, EGF, IGF-1, heparin, hydrocortisone, and ascorbate), and EGM-2 with 2%, 5%, or 10% FBS.

Hybrid Approach

Slabs of aspect ratio 1.5 were cast with the same cell concentrations and fibrin formulation as above. All slabs were cultured for 3 days in defined medium, after which they were cultured for an additional 3 days in either defined medium or EGM-2+.

Fibril Orientation

Alignment of fibrin fibrils in slabs was verified with polarimetry, as previously described (Tower and Tranquillo, 2001). The average retardation value was normalized to slab thickness, yielding birefringence, a measure of fibril alignment.

Microvascular Network Evaluation

Constructs created in 96-well plates were fixed and stained whole for CD31 (Dako). Hoecsht 33342 dye (Invitrogen) labeled the nuclei. Constructs were imaged using an epifluorescence microscope.

Images were automatically thresholded and analyzed using a custom Matlab code. For the purposes of this analysis, a “segment” was defined as a microvessel between two bifurcation points, and a “structure” was defined as a contiguous set of microvessels and could be made up of multiple segments. Alignment was assessed by skeletonizing the network and measuring the length and angle of each segment. An anisotropy index (AI) was defined for each image such that

$$AI = \frac{\sum L_x}{\sum L_y},$$

where L_x and L_y are the components of segment length in the directions parallel and perpendicular to alignment, respectively. The area fraction of the image stained positively for CD31 (“CD31 fraction”) was taken as an indication of HUVEC density. PC density and recruitment levels were also evaluated in Matlab. A GFP-labeled PC was considered recruited if it was in contact with a microvessel. Total cell density measurements were based off of nuclear counts.

Due to the increased density (caused by compaction) and thickness of the slabs relative to the 96-well plate constructs, whole slab imaging was impossible. Instead, thick (40-60 μm) longitudinal sections were cut, stained, and analyzed as above.

Lumen Formation

Frozen cross-sections were stained for CD31. Images were thresholded and potential lumens were detected as dark regions completely surrounded by white (CD31 staining) in a second Matlab code. User input was allowed to either remove non-lumens that were erroneously detected, or connect CD31+ regions to enable the program to detect a lumen it previously missed. Lumen diameters were calculated from areas assuming a circular lumen.

Basement Membrane Staining

Basement membrane deposition was evaluated via immunofluorescent staining (without detergents) of cross-sections using antibodies against collagen IV and laminin (both Abcam). Average pixel intensities for exposure-matched images were calculated via Matlab.

Statistics

Data were analyzed in Minitab using either Student’s t-tests (if only two conditions were evaluated) or one-way ANOVAs with Tukey post-hoc tests. Comparisons to control conditions were performed using Dunnett post-hoc tests.

Results

HUVECs and PCs form highly interconnected microvascular networks in fibrin gel under defined conditions

A small volume gel format (96-well half-area plates) was used to optimize conditions for HUVEC microvascular network formation using defined medium or EGM-2+ with or without co-cultured PCs. Representative images of whole mount CD31 stains and quantification of the network characteristics are shown in Fig. 1. HUVECs co-cultured with PCs in defined medium formed the best network in terms of total length and average connected structure length (a measure of network interconnectivity). Lumens clearly formed, as evidenced by Fig. 1e. Additionally, culture in defined medium produced a greater level of PC recruitment to microvessels than culture in EGM-2+.

Aligned microvascular networks form under defined conditions in slabs of high aspect ratio

The cell-induced gel compaction of fibrin gel slabs containing HUVEC networks was investigated under defined conditions using slabs of varying aspect ratio that were detached at day 3 of culture (i.e. gel compaction began on day 3). Macroscopic images of a slab with an initial aspect ratio of 4.5 and its alignment map are shown in Fig. 2a-b. Representative images of the HUVEC networks are shown in Fig. 2c-d. Slabs with an aspect ratio of 4.5 compacted much more and had more aligned fibrils and microvessels than slabs of aspect ratio 1.5 (Fig. 2e-g). No differences between aspect ratios were observed in total structure length, average structure length, or PC recruitment (Fig 2h-j).

Compaction is detrimental to forming networks but not to previously formed networks

Slabs of aspect ratio 4.5 were cultured in defined medium and detached from the culture plate (enabling compaction to begin) at days 1, 2 or 3. Images of the resulting HUVEC networks are shown in Fig. 3a-d. All of the detached slabs compacted more and were more aligned (Fig. 3e-g) than the day 3 control slabs that were never detached. Additionally the microvessels of the slabs detached at day 1 were more aligned than any other condition. No differences in total structure length or PC recruitment were observed between any of the conditions, but the average structure length was reduced in slabs detached at days 1 or 2 in comparison to controls. Slabs detached at day 2 also had lower average structure length than those detached at day 3. The average structure length of slabs detached at day 3 was not different from controls (Fig. 3h-j).

Slabs of aspect ratio 4.5 detached at day 3 were further analyzed for lumen formation and basement membrane deposition. They were compared to 96-well plate controls (created at the same time and cultured for 3 days) for which the culture conditions were optimized. Representative images of CD31 and collagen IV staining are shown in Fig. 4a-d. Analysis of CD31-stained images revealed that the lumen density, average lumen diameter and the cell density (including both HUVECs and PCs) were increased in the aligned slabs over the controls, although no statistically-significant differences were observed in either CD31+ area fraction or PC density (Fig 4e-i). No differences were observed in total staining intensity for either laminin or collagen IV staining, but laminin staining per cell was decreased in the slabs (Fig. 4j-m).

EGM-2+ improves compaction

Additional medium formulations were tested to determine if they could improve the limited compaction and alignment observed in slabs of aspect ratio 1.5. Slabs were cultured in defined medium for 3 days followed by the test medium for 3 days. Only serum-containing EGM-2+ improved compaction, irrespective of the serum concentration (Fig. S1).

Hybrid approach yields improved networks over defined medium alone

Due to the relatively low compaction and lumen densities observed using defined medium, a hybrid approach was investigated in which slabs (aspect ratio 1.5) were cultured in defined medium for 3 days, detached, and cultured in EGM-2+ for an additional 3 days. Representative images of the HUVEC networks are shown in Fig. 5a-c. Macroscopic images and alignment maps of day 6 slabs cultured in defined medium or EGM-2+ are shown in Fig. 5d-g. In comparison to slabs cultured in defined medium for 3 or 6 days, hybrid slabs compacted more and had higher fibril and microvessel alignment (Fig. 5h-j). In addition, the total structure length (Fig. 5k) and average structure length (Fig. 5l) were the same between the day 6 hybrid slabs and the day 3 control, but reduced for the slabs cultured for 6 days in defined medium; PC recruitment was the same for all conditions (Fig. 5m). Slabs cultured for 3 days in defined medium were used as a baseline control here, representing the microvessel state prior to the test conditions. This enabled the characterization of microvessel growth or regression caused by EGM-2+.

Additional network characteristics were quantified from CD31-stained cross sections. Representative images are shown in Fig. 6a-c. Lumen density was improved in hybrid slabs over the day 3 control (Fig 6d), and mean lumen diameter was increased in day 6 defined medium slabs over the day 3 control (Fig. 6e). The total cell density (based on nuclear counts) was increased in hybrid slabs over all other conditions (Fig. 6f). The area fraction of CD31 staining (reflecting the EC density) was also increased in hybrid slabs over day 6 defined medium slabs (Fig. 6g). No differences were observed in PC density (Fig. 6h). Basement membrane deposition was also examined in immunostained cross sections. Representative images of collagen IV staining are shown in Fig. 6i-k; laminin staining was similar (not shown). A higher total intensity of laminin staining per area was observed in hybrid slabs as compared to day 6 defined medium slabs (Fig. 6l), but this difference did not exist when the staining intensity was normalized to total cell density (Fig. 6m). Total collagen IV staining per area was increased in hybrid slabs over both other conditions (Fig. 6n), but collagen IV per cell was decreased in hybrid slabs in comparison to day 6 defined medium slabs.

Discussion

The achievement of a highly interconnected microvascular network in fibrin gel under defined conditions complements our previously developed type I collagen system (Stratman et al., 2009). It is interesting to note that in the fibrin gel system both the defined medium and the PCs were required to achieve a highly interconnected network; in the collagen gel system PCs were not required for the initial network formation (Stratman et al., 2009). Additionally, networks formed with many EC:PC ratios (data not shown). The presence of PCs increased the total structure length in both media, but to a lesser degree in serum-containing EGM-2+. One possible explanation is that either the proximity of PCs to the ECs or additional factors they provided improved the network formation in the presence of PCs. Additionally, the recruitment of the PCs to the microvessels was higher in defined medium. This may be due to an increase in local gradients of chemokines due to the relative lack of chemokines present in defined medium in comparison to EGM-2+. For example, PDGF-BB, which is known to induce PC recruitment both *in vivo*,and *in vitro* (Bjarnegård et al., 2004; Stratman et al., 2010) is not present in defined medium, but is likely present at a low level in the serum used in EGM-2+.(Kumar, Bennett, & Brody, 1988) Therefore, any PDGF-BB produced by the HUVECs would induce a larger gradient in defined medium than in EGM-2+. Additional experimentation would be necessary in order to fully understand all of these effects, and was beyond the intended scope of this report.

Previous work has shown that the alignment of both matrix and sprouts from EC spheroids in an angiogenic system increases with slab aspect ratio (Morin and Tranquillo, 2011), and that appears to be true in this vasculogenic system as well. However, slabs of aspect ratio 3 in the previous report had 8-fold higher birefringence compared to the slabs of higher aspect ratio (4.5) used here. This is likely due to the relatively low level of gel compaction, which drives alignment (Barocas & Tranquillo, 1997; Morin & Tranquillo, 2011), obtained in defined medium.

The compaction that did occur in defined medium had a deleterious effect on microvascular network formation. Slabs that were detached on days 1 or 2, prior to the completion of network formation, formed some microvessels, but they were not as interconnected as the day 3 controls. Only day 6 slabs that were detached on day 3, after network formation had occurred, were identical to the day 3 controls in every characteristic that was assessed (except alignment). The fact that the total structure length was the same across conditions suggests that any increased matrix density caused by compaction or reduction in local matrix tension caused by detachment from the plate had a minimal effect on microvessel growth. However, the reduced network connectivity observed with premature detachment may be explained by the similar growth direction that would have been prescribed for all of the microvessels due to the increased matrix alignment, reducing the probability that microvessels would connect to nearby microvessels. Another effect observed in slabs detached on varying days is that the network alignment was highest in the slabs detached on day 1. This could be explained by the additional day(s) of compaction-induced alignment experienced by these slabs. Another factor may be that the microvessels of slabs detached at days 1 or 2 were forming as alignment was developing, possibly enabling a greater role for contact guidance-induced alignment (Barocas & Tranquillo, 1997), as compared to the slabs detached at day 3 that largely contained formed microvessels that were reoriented with the compacting network of ECM fibers.

Despite the relatively low levels of compaction observed in defined medium, the compaction that occurs in slabs of aspect ratio 4.5 detached at day 3 is sufficient to achieve alignment of the microvascular network. Because this fibrin gel system was optimized for the 96 well plate constructs, comparison of the whole mount network characteristics between the aligned slabs and the 96 well plate constructs was of interest. The network characteristics obtained from sections of both sample types from the same experiment (Fig. 4) demonstrate improvement in the microvascular characteristics in the slabs over the 96-well plate constructs. The cause of this improvement cannot be determined due to the many differences between the conditions, including the sample geometry, the day of harvest, and the level of compaction. Additionally, the deposition of basement membrane was assessed in both sample types. Although there was no difference in total deposition of either laminin or collagen IV, a reduction in laminin staining per cell was observed in the slabs, suggesting that each cell was producing less matrix. This is particularly interesting due to the fact that the slabs were cultured for 3 days longer than the 96-well plate constructs.

Additional experiments were completed to determine whether or not additional factors could be added to the defined medium to induce more gel compaction. Higher levels of compaction would be desirable to increase the alignment and mechanical strength of engineered tissues. EGM-2+ was used as a positive control because it caused a high level of compaction in preliminary experiments. Despite the fact that TGF-β1 is known to increase cell contractility (Grinnell and Ho, 2002; Grouf et al., 2007), the addition of TGF-β1 to defined medium did not increase compaction. Similarly, the addition of EGM-2 bulletkit components (except serum) to the defined medium did not increase compaction. While EGM-2+ induced extensive compaction, varying the amount of serum did not affect the degree of compaction. It is unclear which component(s) of EGM-2+ induced high levels of

compaction, and a more high-throughput method than is currently available would be required to answer this question.

Because serum-containing medium was required to achieve extensive compaction, a hybrid approach was examined in which slabs of aspect ratio 1.5 were cultured in defined medium for 3 days followed by EGM-2+ for 3 days. The microvascular networks thus formed prior to compaction induction by EGM-2+. This method succeeded in producing highly aligned microvascular networks; not only was the alignment of both fibrils and microvessels stronger in these hybrid slabs than that of slabs cultured entirely in defined medium (Fig. 5), but it also appeared to be stronger than that of defined medium slabs of aspect ratio 4.5 cultured in defined medium (Fig. 2). The fact that the network properties did not vary between the hybrid and day 3 control slabs suggests that the addition of EGM-2+ after network formation did not have a detrimental effect. The hybrid approach was not compared to a day 6 condition of EGM-2+ only medium because of results reported above: 96-well plate samples demonstrated that culture in EGM-2+ does not yield well-formed structures, and slabs indicated that gel compaction has a detrimental effect on further structure formation.

Not only did the addition of EGM-2+ lack detrimental effects, it had a beneficial effect on lumen density, raising the density within the physiologic range for dermis (Debbabi et al., 2006). EGM-2+ also increased the overall cell density in comparison to the other conditions. This cell density is attributable to the HUVECs as differences in PC density between conditions were not statistically significant. The density of basement membrane (both laminin and collagen IV) was increased in hybrid slabs; however this difference disappeared (laminin) or reversed (collagen IV) when the staining intensity was normalized to cell number, suggesting that the cellular production of these proteins was the same or lower in the EGM-2+. The high level of basement membrane proteins deposited by day 3 may be part of the reason that these microvascular networks were relatively stable under compaction and the change of medium type, as basement membrane is thought to be a major contributor to microvessel stability *in vivo* (Allt & Lawrenson, 2001).

These results have demonstrated two methods for forming highly interconnected, aligned microvascular networks within mechanically-constrained fibrin gel. The method involving only defined medium results in slabs with relatively low levels of compaction, but would be useful to EC biologists requiring full control over the culture conditions. The hybrid approach, although it relinquishes some control over the culture conditions, yields slabs with relatively high levels of compaction and resultant network alignment, which is of interest to tissue engineers. Therefore, the HUVEC and PC co-culture fibrin gel system developed here has the potential for widespread use.

Supplementary Material

Refer to Web version on PubMed Central for supplementary material.

Acknowledgments

The authors thank Pat Schaeffer for histological assistance.

Funding

This work was supported by the National Institutes of Health [R01 HL108670 to RTT]; and the American Heart Association [11PRE7610056 to KTM].

Abbreviatons

EC	endothelial cell
HUVEC	human umbilical vein endothelial cell
MSC	mesenchymal stem cell
PC	pericyte

References

Allt G, Lawrenson JG. Pericytes: cell biology and pathology. Cells, tissues, organs. 2001; 169:1–11. [PubMed: 11340256]

Barocas VH, Tranquillo RT. An anisotropic biphasic theory of tissue-equivalent mechanics: the interplay among cell traction, fibrillar network deformation, fibril alignment, and cell contact guidance. J. Biomech. Eng. 1997; 119:137–145. [PubMed: 9168388]

Benjamin LE, Hemo I, Keshet E. A plasticity window for blood vessel remodelling is defined by pericyte coverage of the preformed endothelial network and is regulated by PDGF-B and VEGF. Development. 1998; 125:1591–1598. [PubMed: 9521897]

Bjarnegård M, Enge M, Norlin J, Gustafsdottir S, Fredriksson S, Abramsson A, Takemoto M, Gustafsson E, Fässler R, Betsholtz C. Endothelium-specific ablation of PDGFB leads to pericyte loss and glomerular, cardiac and placental abnormalities. Development. 2004; 131:1847–1857. [PubMed: 15084468]

Caulfield JB, Janicki JS. Structure and function of myocardial fibrillar collagen. Technol. Health Care. 1997; 5:95–113. [PubMed: 9134622]

Chen X, Aledia AS, Popson SA, Him L, Hughes CCW, George SC. Rapid anastomosis of endothelial progenitor cell-derived vessels with host vasculature is promoted by a high density of cotransplanted fibroblasts. Tissue Eng. Part A. 2010; 16:585–594. [PubMed: 19737050]

Clark RA, Nielsen LD, Welch MP, McPherson JM. Collagen matrices attenuate the collagen-synthetic response of cultured fibroblasts to TGF-beta. J. Cell Sci. 1995; 108:1251–1261. [PubMed: 7622608]

Collen A, Hanemaaijer R, Lupu F, Quax PH, van Lent N, Grimbergen J, Peters E, Koolwijk P, van Hinsbergh VW. Membrane-type matrix metalloproteinase-mediated angiogenesis in a fibrin-collagen matrix. Blood. 2003; 101:1810–1817. [PubMed: 12393408]

Davis GE, Camarillo CW. An alpha 2 beta 1 integrin-dependent pinocytic mechanism involving intracellular vacuole formation and coalescence regulates capillary lumen and tube formation in three-dimensional collagen matrix. Exp. Cell Res. 1996; 224:39–51. [PubMed: 8612690]

Davis, George E.; Stratman, AN.; Sacharidou, A.; Koh, W. Molecular basis for endothelial lumen formation and tubulogenesis during vasculogenesis and angiogenic sprouting. Intl. Rev. Cell Mol. Biol. 2011; 288:101–165.

Debbabi H, Uzan L, Mourad JJ, Safar M, Levy BI, Tibiriçà E. Increased skin capillary density in treated essential hypertensive patients. Am. J. Hypertens. 2006; 19:477–483. [PubMed: 16647618]

Ghajar CM, Chen X, Harris JW, Suresh V, Hughes CC, Jeon NL, Putnam AJ, George SC. The effect of matrix density on the regulation of 3-D capillary morphogenesis. Biophys. J. 2008; 94:1930–1941. [PubMed: 17993494]

Grainger SJ, Putnam AJ. Assessing the permeability of engineered capillary networks in a 3D culture. PloS One. 2011; 6:e22086. [PubMed: 21760956]

Grassl ED, Oegema TR, Tranquillo RT. Fibrin as an alternative biopolymer to type-I collagen for the fabrication of a media equivalent. J. Biomed. Mater. Res. 2002; 60:607–612. [PubMed: 11948519]

Grinnell F, Ho C-H. Transforming growth factor beta stimulates fibroblast-collagen matrix contraction by different mechanisms in mechanically loaded and unloaded matrices. Exp. Cell Res. 2002; 273:248–255. [PubMed: 11822880]

Grouf JL, Throm AM, Balestrini JL, Bush KA, Billiar KL. Differential effects of EGF and TGF-beta1 on fibroblast activity in fibrin-based tissue equivalents. Tissue Eng. 2007; 13:799–807. [PubMed: 17346099]

Hellström M, Gerhardt H, Kalén M, Li X, Eriksson U, Wolburg H, Betsholtz C. Lack of pericytes leads to endothelial hyperplasia and abnormal vascular morphogenesis. J. Cell Biol. 2001; 153:543–553. [PubMed: 11331305]

Kaully T, Kaufman-Francis K, Lesman A, Levenberg S. Vascularization-The Conduit to Viable Engineered Tissues. Tissue Eng. Part B. 2009; 15:159–169.

Koh W, Stratman AN, Sacharidou A, Davis GE. In vitro three dimensional collagen matrix models of endothelial lumen formation during vasculogenesis and angiogenesis. Methods Enzymol. 2008; 443:83–101. [PubMed: 18772012]

Korff T, Augustin HG. Tensional forces in fibrillar extracellular matrices control directional capillary sprouting. J. Cell Sci. 1999; 112:3249–3258. [PubMed: 10504330]

Kumar, R.; Bennett, R.; Brody, A. An enzyme immunoassay for platelet-derived growth factor (PDGF): Application to the measurement of macrophage-derived PDGF. In: Powanda, MC., editor. Monokines and Other Non-Lymphocytic Cytokines. Alan R. Liss, Inc.; New York: 1988. p. 393-396.

Maciag T, Cerundolo J, Ilsley S, Kelley PR, Forand R. An endothelial cell growth factor from bovine hypothalamus: identification and partial characterization. Proc. Natl. Acad. Sci. U.S.A. 1979; 76:5674–5678. [PubMed: 293671]

Morin KT, Tranquillo RT. Guided sprouting from endothelial spheroids in fibrin gels aligned by magnetic fields and cell-induced gel compaction. Biomaterials. 2011; 32:6111–6118. [PubMed: 21636127]

Nakatsu MN, Hughes CCW. An optimized three-dimensional in vitro model for the analysis of angiogenesis. Methods Enzymol. 2008; 443:65–82. [PubMed: 18772011]

Price GM, Wong KHK, Truslow JG, Leung AD, Acharya C, Tien J. Effect of mechanical factors on the function of engineered human blood microvessels in microfluidic collagen gels. Biomaterials. 2010; 31:6182–6189. [PubMed: 20537705]

Rao RR, Peterson AW, Ceccarelli J, Putnam AJ, Stegemann JP. Matrix composition regulates three-dimensional network formation by endothelial cells and mesenchymal stem cells in collagen/fibrin materials. Angiogenesis. 2012; 15:253–264. [PubMed: 22382584]

Stratman AN, Davis GE. Endothelial cell-pericyte interactions stimulate basement membrane matrix assembly: influence on vascular tube remodeling, maturation, and stabilization. Microsc. Microanal. 2012; 18:68–80. [PubMed: 22166617]

Stratman AN, Davis MJ, Davis GE. VEGF and FGF prime vascular tube morphogenesis and sprouting directed by hematopoietic stem cell cytokines. Blood. 2011; 117(14):3709–3719. [PubMed: 21239704]

Stratman AN, Malotte KM, Mahan RD, Davis MJ, Davis GE. Pericyte recruitment during vasculogenic tube assembly stimulates endothelial basement membrane matrix formation. Blood. 2009; 114:5091–5101. [PubMed: 19822899]

Stratman AN, Schwindt AE, Malotte KM, Davis GE. Endothelial-derived PDGF-BB and HB-EGF coordinately regulate pericyte recruitment during vasculogenic tube assembly and stabilization. Blood. 2010; 116:4720–4730. [PubMed: 20739660]

Syedain ZH, Lahti M, Johnson SL, Robinson PS, Ruth GR, Bianco RW, ranquillo RT. Implantation of a Tissue-engineered Heart Valve From Human Fibroblasts Exhibiting Short Term Function in the Sheep Pulmonary Artery. Cardiovasc. Eng. Technol. 2011; 2:101–112.

Syedain ZH, Meier LA, Lahti M, Johnson SL, Hebbel RP, Tranquillo RT. Implantation of completely biological, aligned engineered arteries pre-made from allogeneic fibroblasts in a sheep model. Nature Med. In Revision.

Tower TT, Tranquillo RT. Alignment maps of tissues: II. Fast harmonic analysis for imaging. Biophys. J. 2001; 81:2964–2971. [PubMed: 11606306]

Vera RH, Genove E, Alvarez L, Borros S, Kamm R, Lauffenburger D, Semino CE. Interstitial Fluid Flow Intensity Modulates Endothelial Sprouting in Restricted Src-Activated Cell Clusters During Capillary Morphogenesis. Tissue Eng. Part A. 2008; 15:175–185.

Zheng Y, Chen J, Craven M, Choi NW, Totorica S, Diaz-Santana A, Kermani P, Hempstead B, Fischbach-Teschl C, López J, Stroock AD. In vitro microvessels for the study of angiogenesis and thrombosis. Proc. Natl. Acad. Sci. U.S.A. 2012; 109:9342–9347. [PubMed: 22645376]

Research Highlights

- Highly interconnected microvessels were formed in fibrin gel using defined medium.
- The microvessels were highly aligned via constrained cell-induced gel compaction.
- Minimal compaction occurred in defined medium compared to medium with serum.
- Defined medium followed by medium with serum yielded the most aligned microvessels.

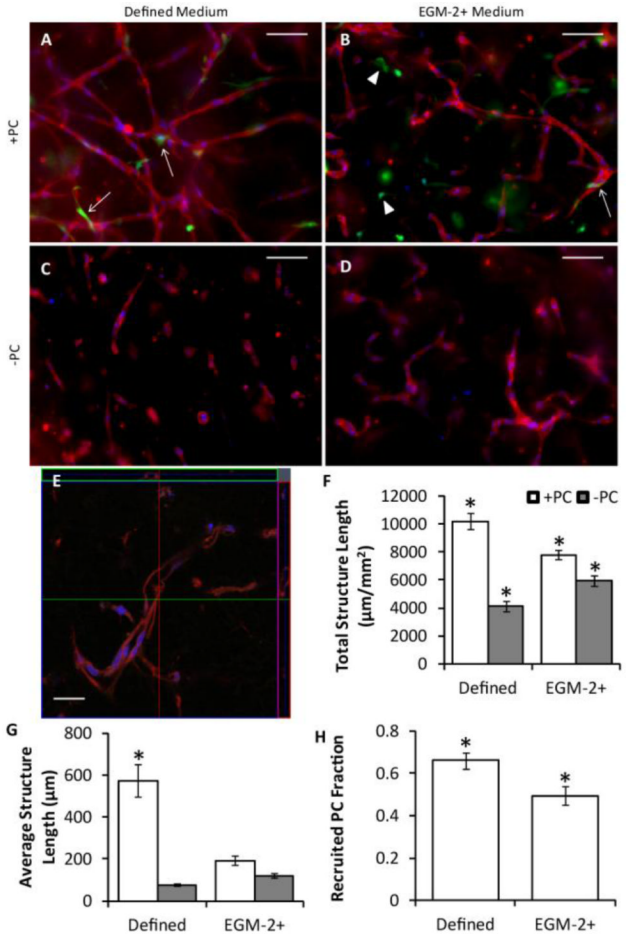

Figure 1.

Vasculogenesis in 96-well plate constructs. (A-D) Representative images of whole mount CD31 stains of HUVECs (red) with (A-B) or without (C-D) PCs (green) in defined medium (A,C) or EGM-2+ (B,D) after 3 days of culture. Nuclei are stained blue. Arrows indicated recruited PCs, and arrowheads indicated PCs that were not recruited. Scalebars = 100 μm. (E) Confocal z-stack of a construct similar to that of (A). The large image is one slice of the stack, and the top and right images represent optical cross-sections through the sample at the green and red lines. Scalebar = 30 μm. (F-H) Quantitation of microvessel network properties. HUVECs grown with PCs in defined medium demonstrated improved total structure length (F), average structure length (G), and PC recruitment (H) over all other conditions. *$p < 0.05$ in comparison to all other conditions.

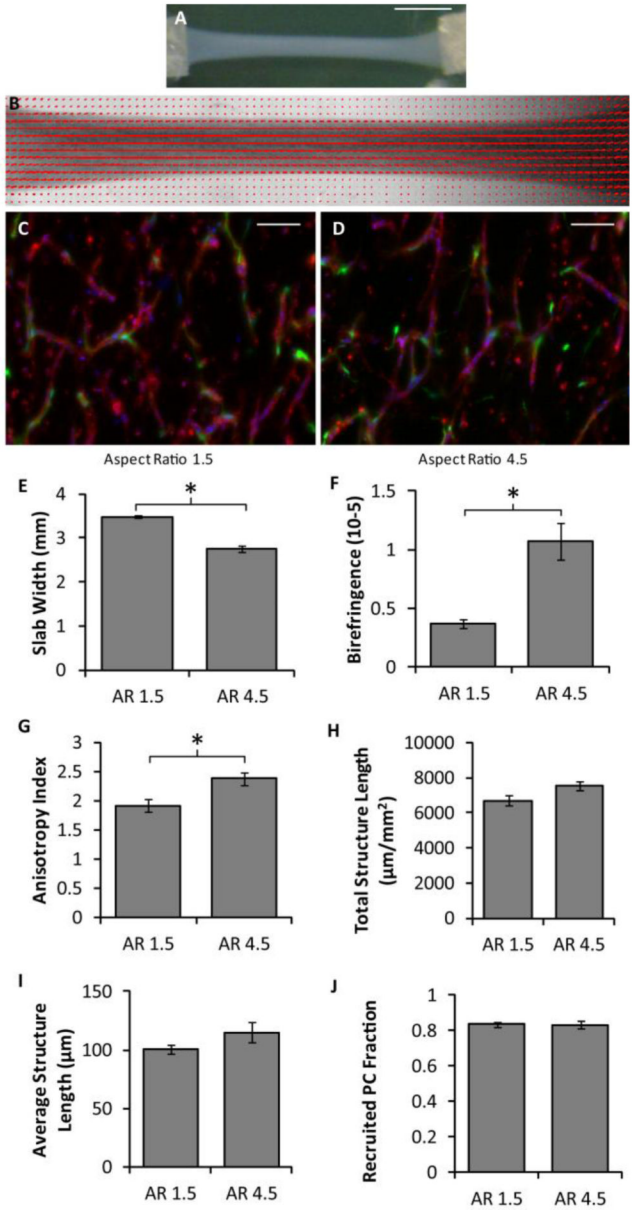

Figure 2.

Effect of slab aspect ratio on vasculogenesis and microvessel alignment. (A) Macroscopic image of a slab with an aspect ratio of 4.5 after compaction in defined medium. Scalebar = 5 mm. (B) Alignment map of the compacted slab shown in (A). The red segments indicate the local strength and direction of fibril alignment. (C-D) Representative images of CD31-stained (red) thick longitudinal sections of slabs with aspect ratios of 1.5 (C) and 4.5 (D). The long axes of the slabs are vertical. PCs are green and nuclei are blue. Scalebars = 100 μm. (E-G) Slab compaction (width at the middle of the slab; E), Fibrin fibril alignment (birefringence; F), and microvessel alignment (anisotropy index; G) show that the slabs with higher aspect ratio that compacted more were also more aligned. (H-J) No differences were observed between slabs of different aspect ratio for a number of microvessel characteristics, including total vessel length per area (H), the average structure length (I), and the recruited PC fraction (J). *$p < 0.05$.

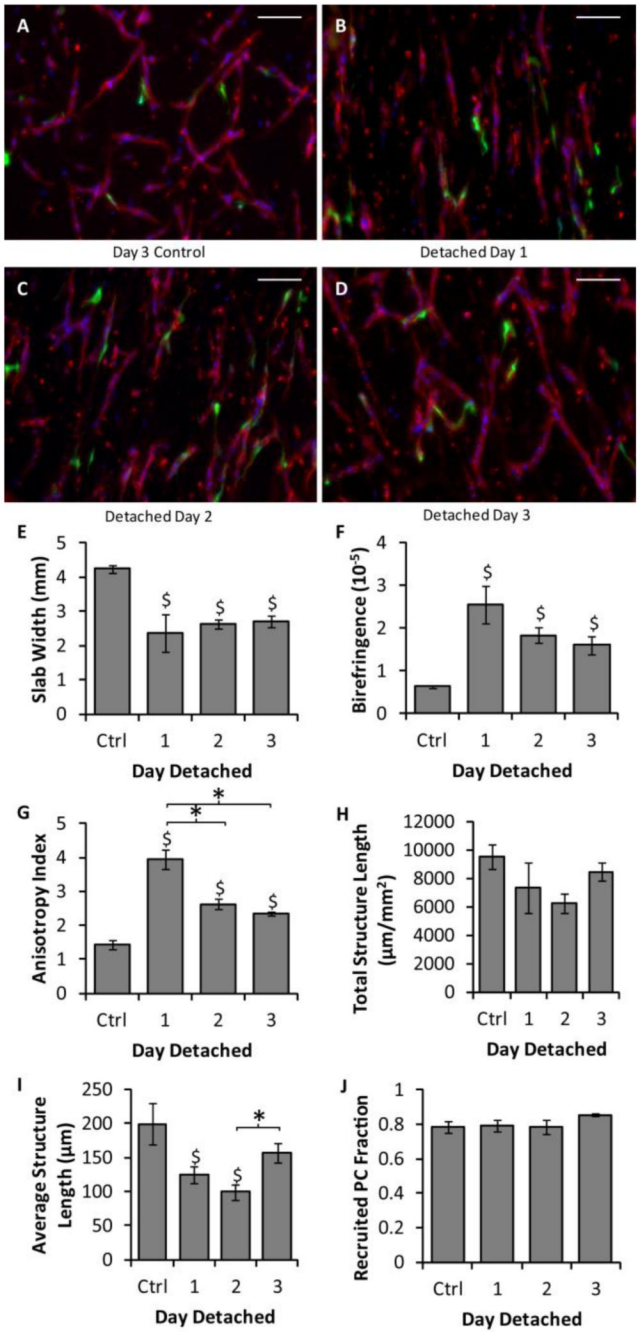

Figure 3.

Effect of slab detachment day on vasculogenesis and microvessel alignment. (A-D) Representative images of CD31 stains (red) of thick longitudinal sections of slabs cultured in defined medium that were never detached and harvested at day 3 (A), or that were detached at day 1 (B), day 2 (C), or day 3 (D) and harvested at day 6. The long axes of the slabs are vertical. PCs are green and nuclei are blue. Scalebars = 100 μm. (E-G) Measures of slab compaction (width at the middle of the slab; E), fibrin fibril alignment (birefringence; F), and microvessel alignment (anisotropy index; G) indicated that all of the detached slabs compacted and that both the fibrin and the microvessels became aligned. (H-J) Measures of microvessel properties, including total microvessel length per area (H), average structure

length (I), and PC recruitment (J), suggested that the aligned microvascular networks present in the slabs detached on day 3 were equivalent to those of the day 3 controls. *$p < 0.05$. \$$p < 0.05$ in comparison to the control.

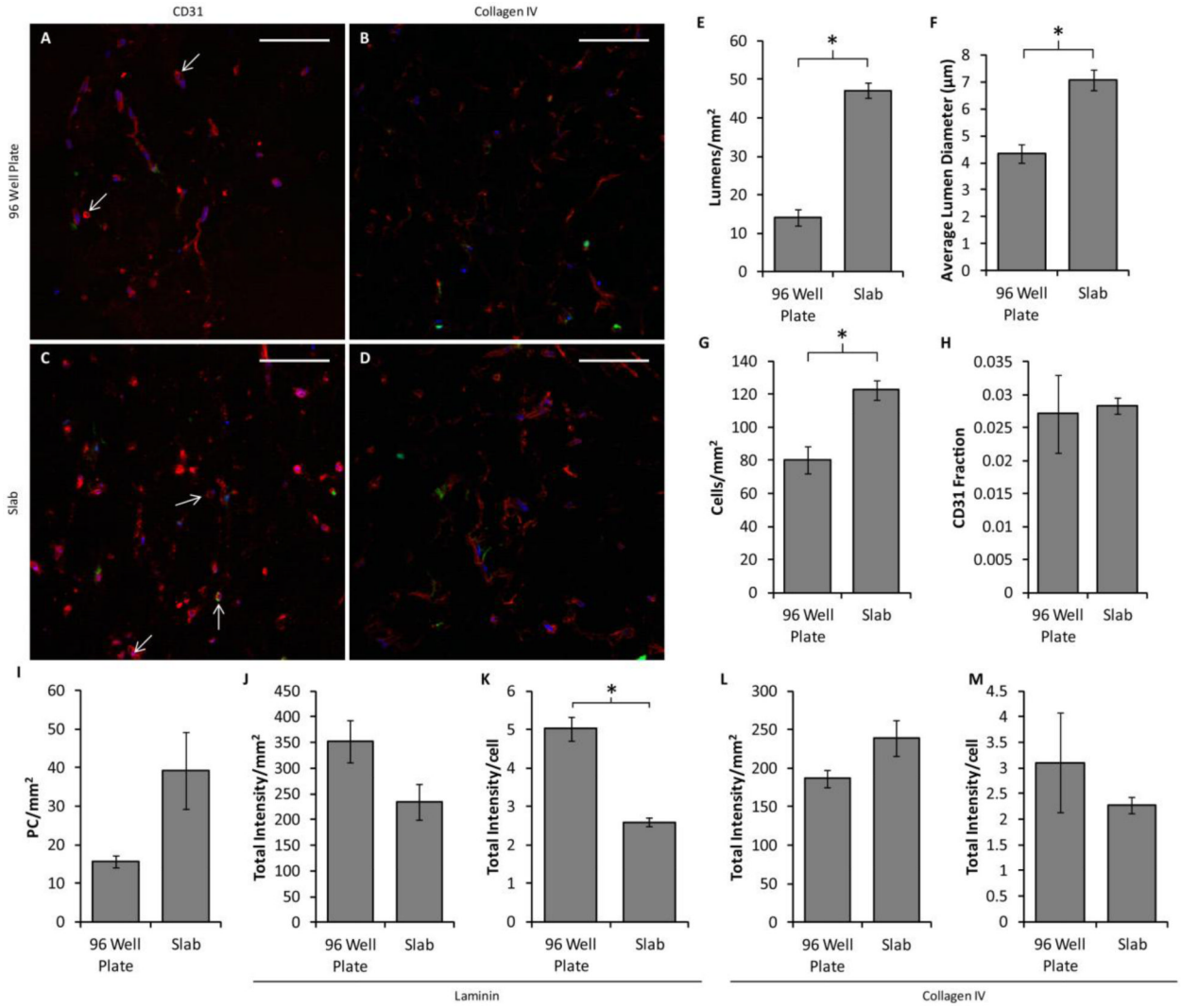

Figure 4.

Comparison of vasculogenesis between 96-well plate constructs and slabs. (A-D) Representative images of cross sections of constructs created in 96 well plates (A-B) or in the slab geometry (C-D) and cultured in defined medium, stained for either CD31 (A,C) or collagen IV (B,D) in red. PCs are green and nuclei are blue. Arrows indicate the location of lumens. Scalebars = 100 μm. (E-H) Quantification of microvessel properties from CD31-stained images, including lumen density (E), average lumen diameter (F), the total cell density (G), the area fraction of CD31 staining (indicative of EC density; H), and the PC density (I). The slabs contained more and larger lumens as well as a higher total cell density, although no differences were observed among conditions for either CD31 fraction or PC density. (J-M) Basement membrane deposition. No differences were observed in total staining intensity of sections stained for laminin (J) or collagen IV (L). However, laminin staining intensity normalized to cell density was reduced in the slab geometry (K). No difference was observed in collagen IV staining per cell. *$p < 0.05$.

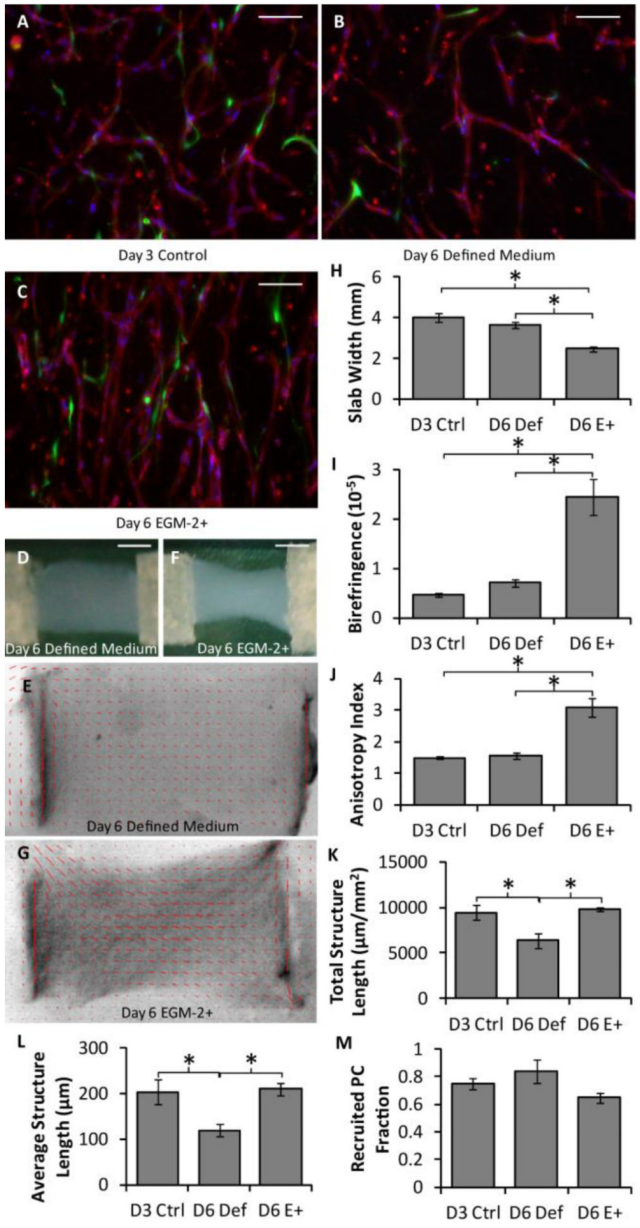

Figure 5.

Analysis of the hybrid approach based on whole mount microvessel properties. (A-C) Representative images of thick longitudinal sections of slabs using the hybrid approach, in which some slabs were harvested at day 3 (A) and others were cultured for an additional 3 days in either defined medium (B) or EGM-2+ (C). HUVECs were stained for CD31 (red), PCs were GFP-labeled (green) and nuclei were stained blue. The long axes of the slabs are vertical. Scalebars = 100 μm. (D-G) Macroscopic images (D,F) and alignment maps (E,G) of slabs cultured in defined medium (D-E) or EGM-2+ (F-G). The red segments in the alignment maps indicate the local strength and direction of fibril alignment. (H-J) Alignment and compaction parameters indicated that the slabs cultured in EGM-2+ had higher fibrin fibril alignment (birefringence; H), compacted more (smallest width at the middle of the slab; I), and had higher microvessel alignment (anisotropy index; J) than slabs cultured in defined medium. (K-M) Microvascular network characteristics, including total microvessel

length per area (K) and average structure length (L), were similar between slabs cultured in EGM-2+ and the control slabs, but reduced in slabs cultured in defined medium. PC recruitment (M) was similar across all conditions. *$p < 0.05$.

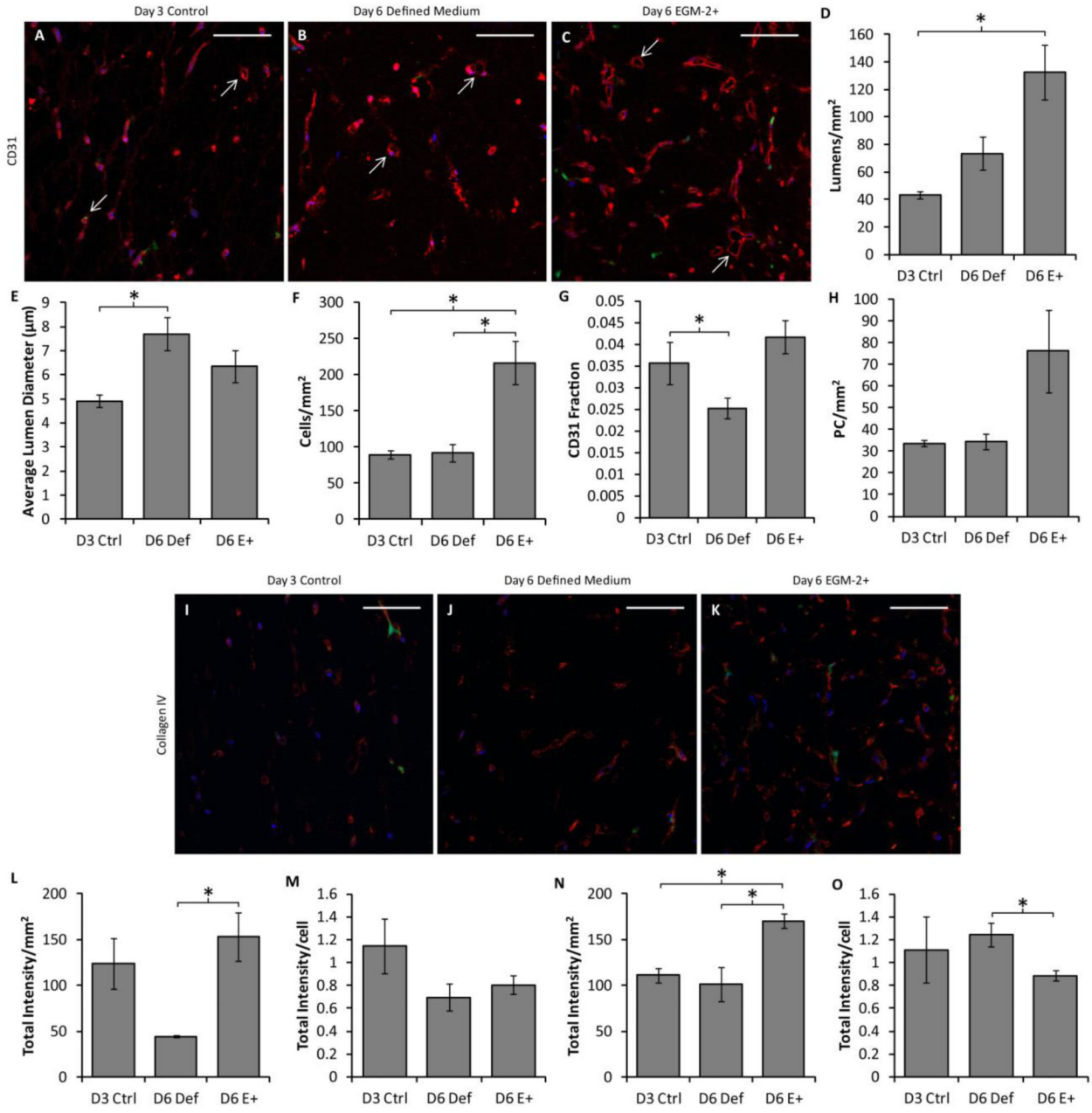

Figure 6.

Analysis of the hybrid approach based on cell densities and basement membrane deposition. CD31, laminin and collagen IV staining of slab cross sections was performed. (A-C) Representative CD31 staining (red) of slabs cultured in defined medium for 3 days (A), 6 days (B) or defined medium for 3 days followed by EGM-2+ for 3 days (C). PCs are green and nuclei are blue. Arrows indicate examples of lumens that were characterized. Scalebars = 100 μm. (D-H) Quantification of sections. The lumen density was improved in hybrid slabs over the control (D), and the average lumen diameter was larger in day 6 defined medium slabs (E). The cell density (F) was highest in the hybrid slabs. The area fraction of CD31 staining (indicative of EC density; G) was increased in hybrid slabs over day 6 defined medium slabs, but the PC density (H) was constant across conditions. (I-K) Representative collagen IV staining of control (I), defined medium (J), and hybrid (K) slabs.

Laminin staining was similar and therefore is not shown. (L-O) Quantification of basement membrane staining. More total laminin staining was present per area in hybrid slabs than day 6 defined medium slabs (L); however no difference was observed in staining intensity per cell (M). A similar trend was observed for collagen IV staining, except that the staining intensity per cell was decreased in hybrid slabs (N-O).